Integrating Air Systems in Aircraft Multidisciplinary Design Optimization

Ali Tfaily

Department of Mechanical Engineering

McGill University, Montreal

August 2018

A thesis submitted to McGill University in partial fulfillment of the requirements of the degree of Master of Engineering

ACKNOWLEDGEMENTS

I would like to thank my supervisor, Prof. Michael Kokkolaras, for his support and guidance throughout my time as his student. I am honored to have worked along a supervisor that always helped me in my work and even my personal life.

I am grateful to members of Bombardier's Advanced Product Development department for their insights on aircraft design and optimization. Special acknowledgment is given to the Thermodynamics department at Bombardier Product Development Engineering, namely Sebastien Beaulac, Hongzhi Wang, Jean-Francois Reis, and Emmanuel Germaine, who provided expertise that greatly assisted this research. I would also like to thank Jean Brousseau for sharing his knowledge on air systems design.

I am very grateful to John Ferneley, Susan Liscouët-Hanke, Pat Piperni, and Fassi Kafyeke who were supportive of my career goals and provided me the means to pursue these goals.

Finally, I am grateful to my friends and family for their constant support and encouragement throughout the ups and downs of my studies.

ABSTRACT

The strong interactions between aircraft and air systems necessitate the integration of the latter to multidisciplinary design optimization (MDO) considerations of the former. This research presents such a methodology considering environmental control and ice protection systems. These systems consume pressurized bleed air from the aircraft's engines to perform their respective functions. We first describe the models used to predict the behavior of these systems and then propose different approaches to their integration into an existing aircraft MDO environment. A business jet test case was studied using the developed methodology. The comparison of MDO results obtained with and without the considered air systems demonstrate the impact on optimal aircraft design and confirm the importance of integrating air systems in the aircraft MDO environment in early design stages.

Table of Contents

List of Tables

List of Figures

Nomenclature

Acronyms

ACM	Air cycle machine
ECS	Environmental control system
FAA	Federal Aviation Administration
FAR	Federal Aviation Regulations
HP	High pressure
MDO	Multidisciplinary design optimization
WIPS	Wing ice protection system

Symbols

C_p	Air specific heat
E_m	Total water catch efficiency
HL_{solar}	Solar heat loads
HL_{Crew}	Crew heat loads
HL_{Pax}	Passenger heat loads
HL_{Ext}	External heat loads
$MACH$	Flight Mach number
N_{crew}	Number of crew members
N_{pax}	Number of passengers
Q	Cabin or cockpit heat load
m	Air mass flow rate

M	Total water catch per ft of span
$S_{windows}$	Cabin window area
$S_{windshield}$	Cockpit windshield area
$T_{cockpit}$	Cockpit target temperature
T_{cabin}	Cabin target temperature
$T_{ambient}$	Ambient temperature
T_{skin}	Aircraft skin temperature
T_{zone}	Temperature in the studied zone (cabin or cockpit)
UA_{sk}	Thermal conductiveness of the aircraft skin
φ	Solar flux
ΔT	Temperature difference between air supply and zonal temperature
E_m	Total water catch efficiency
LWC	Liquid water content
v	Airspeed
B	Airfoil maximum thickness
$(\rho g)_o$	Ambient air density
L_x	Length of protected surface
C_o:	External film conductance per ft of span of protected surface
q	Heat flow
$\dot{m}_{WIPS}$	WIPS mass flow rate requirement
ε_{sk}	Thermal efficiency of protected skin
T_{WIPS}	Temperature of bleed air within the ice protection system

T_{sk}	Wing skin temperature
$P_{PCE,diss}$	Heat dissipated through the precooler
$\dot{m}_{hot\ side}$	Hot side mass flow rate
T_{bleed}	Bleed temperature
$T_{regulated}$	Regulated bleed temperature by precooler
$C_{d,air}$	Additional drag counts due to air systems
$K_{d,RAM}$	Factor for drag cause by RAM air
$\dot{m}_{RAM}$	Ram air mass flow rate during cruise
$K_{d,PCE}$	Factor for drag caused by precooler exhaust
$\dot{m}_{PCE}$	Total mass flow rate passing through precooler including hot and cold sides

1. INTRODUCTION

Aircraft design is a long iterative process due to the complex interactions of the disciplines within. Aircraft manufacturers use a stage gate approach to the product development process starting from need identification and conceptual design to program certification and entry-into-service [1]-[2]. Aircraft conceptual design has proven to have a significant impact on the success and the overall cost of the product as shown in Figure 1 where design ease of change accompanied by the minimal cost incurred necessitate increasing the maturity of the product during conceptual design.

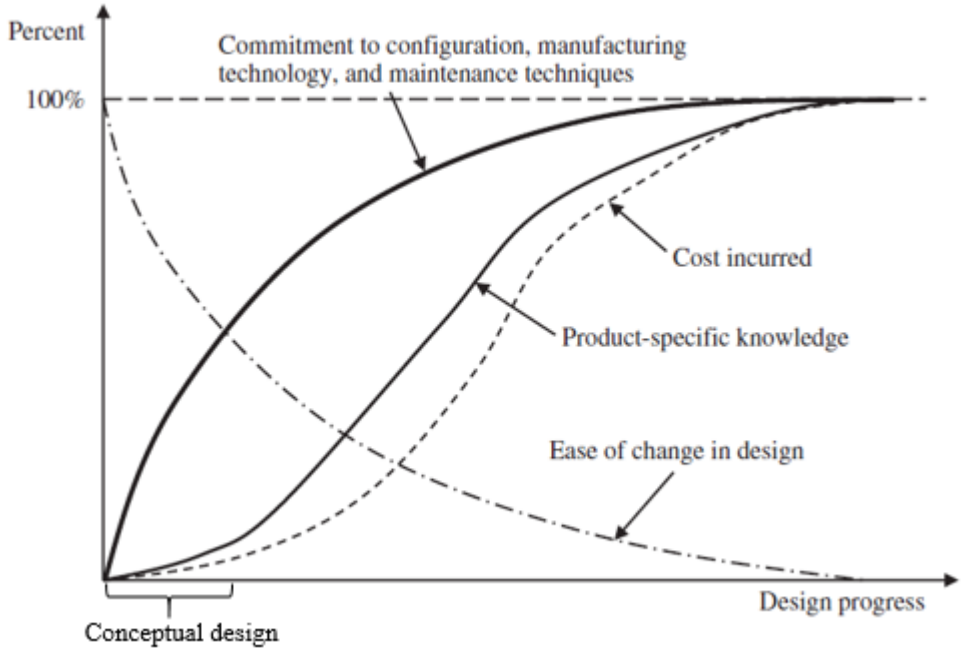

Figure 1: Impact of different aircraft design stages on cost, maturity, ease of change in design, and configuration commitment (adapted from [4])

Historically during conceptual design, aircraft manufacturers focused on a certain number of disciplines that had a significant impact on aircraft weight and performance. This said approach allowed for a shorter design timeframe during concept definition, however this method could lead to numerous issues in the subsequent design stages, specifically regarding systems integration as discussed in [3]. The proposed strategy demonstrates the need for including additional disciplines to be studied during aircraft conceptual design.

The addition of disciplines to the conceptual design process calls for the use of techniques to simplify and accelerate that process. These techniques are called multidisciplinary analysis or more commonly multidisciplinary design optimization (MDO). Aircraft multidisciplinary design optimization has been in development for a number of years with an increasing number of disciplines included in the formulated problems [2]-[9].

Air systems were highlighted as possible candidates to be included in aircraft MDO formulations due to the significant impact of aircraft design and engine bleed characteristics on air systems, and the effect of bleed air on engine performance [10]. Bleed air systems typically include environmental control systems, wing and engine anti-icing systems, engine start, thrust reversers, hydraulic systems, and fuel tank inerting systems [11]. The focus for this research is on environmental control systems and wing ice protection systems as well as the pneumatic system components needed to deliver bleed air from the aircraft engines.

This work builds on an existing aircraft MDO environment that already includes models for several disciplines including some interfacing with air systems. The existing MDO environment was built using the Dassault Systemes Isight software.

The objectives of this research can be summarized as follows:

- Include aircraft weight and performance sensitivities due to changes in air system design parameters in aircraft multidisciplinary design optimization.
- Study the sensitivity of environmental control system performance due to changes in engine bleed characteristics during aircraft conceptual design.
- Study the sensitivity of wing ice protection performance due to changes in wing design and to changes in engine bleed characteristics during aircraft conceptual design.
- Achieve a more mature aircraft design at conceptual definition by reducing the risk of issues that might arise due to air systems design constraints.

2. LITERATURE REVIEW

Aircraft multidisciplinary design optimization has been in development for a number of years with an increasing number of disciplines included in the formulated problems [2]-[9]. Reference [12] reports the integration of landing gear design to aircraft MDO by considering conceptual design models. The impact of landing gear design on aircraft MDO is presented in [13].

An integrated set of models for all major aircraft systems (including air systems) to consider in the conceptual design stage for trade studies and aircraft level architecture definition is discussed in [14].

Models for disciplines within air systems have been developed and used for purposes such as performance, simulation, and diagnostics [12]-[19], [24].

A methodology to optimize weight and entropy generation of an environmental control system for a given aircraft configuration is presented in [17].

Methods to predict ice catch on aircraft wings have been developed with ranging levels of fidelity such as low fidelity methods in [23] and [32] and higher fidelity methods in [29]-[31]. Current higher fidelity methods for air systems sizing and simulation are not suitable for aircraft conceptual design due to high run-time and computing power needs.

Several methods and techniques for implementation of MDO on aircraft design have been studied [25]-[28]. A methodology to integrate air systems in aircraft MDO within conceptual design had not been investigated.

3. AIR SYSTEMS MODELING

Modeling efforts conducted for this work aimed at including air systems-related disciplines into the existing MDO environment. In this section, the modeling approach for the environmental control system, the wing ice protection system, and the pneumatic system is described. The models were built into Dynamic Java code built into the Isight framework of the existing MDO environment.

3.1 Architecture Assumptions

This research studies a fixed aircraft level architecture that is described in this section along with a description of the air systems studied. Figure 2 shows a simplified schematic describing the aircraft air systems top level architecture assumed. The studied air systems are considered to be pneumatic and driven by bleed air from the aircraft engines.

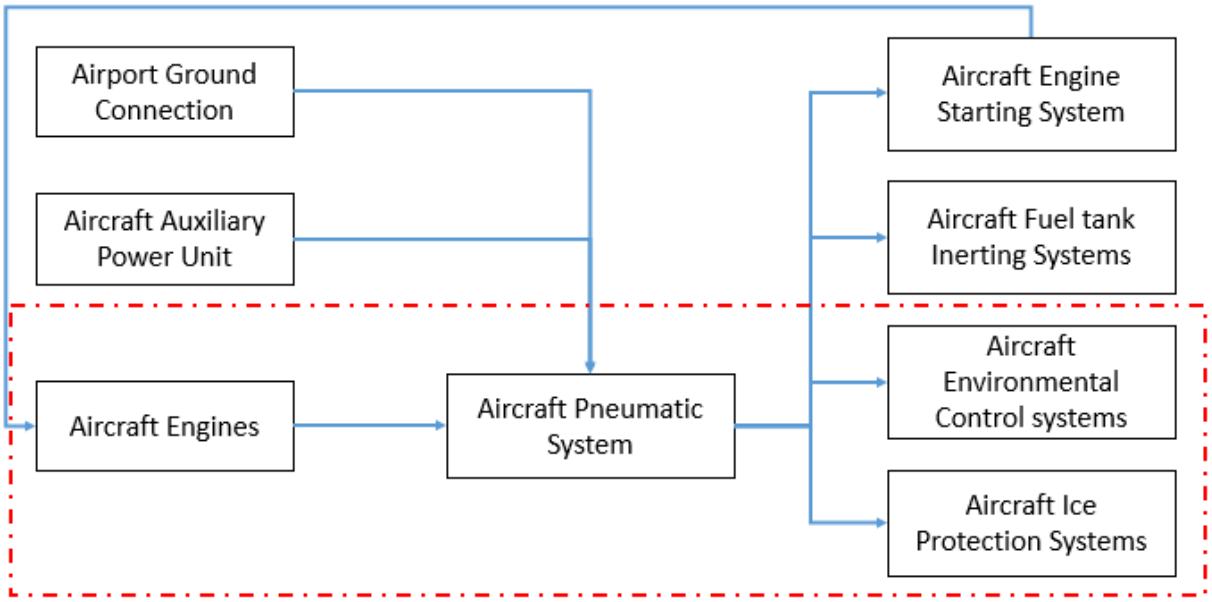

Figure 2: Typical aircraft air systems architecture showing the studied subsystems of this research (enclosed in dashed box)

Modern transport aircraft use turbofan engines that power all of the aircraft systems whether by providing mechanical energy to drive hydraulic and electrical systems or bleed air to drive air systems. Engines power air systems by supplying high-pressure bleed air extracted using bleed ports located usually at 2 different engine compressor stages. An aircraft's pneumatic system transports this bleed air between different systems, and in some aircraft adjusts the temperature of bleed air when a precooler is used. An example of a typical bleed air system is shown in Figure 3 where bleed air is extracted from different compressor stages within the engine core and then supplied to air service consumer systems such as the environmental control system and the ice protection system.. Note the hashed box represents a precooler that uses engine fan air to cool down engine bleed air before supplying it to consumer systems.

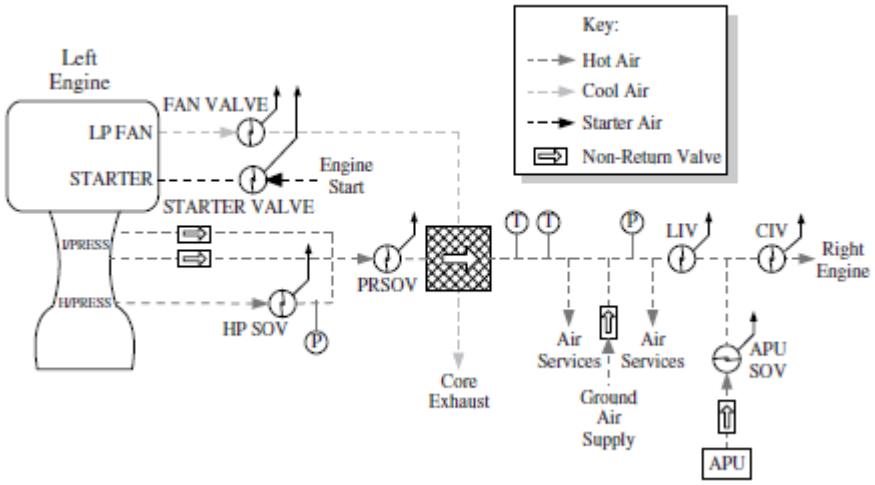

Figure 3: Typical aircraft pneumatic system [11].

Environmental control systems are responsible to control the environment inside the aircraft's cabin, cockpit, and other pressurized areas such as baggage bays and underfloor avionics bays. The environmental control system ensures temperature, pressure, and ventilation targets are met within each controlled zone. Figure 4 shows an example of how an environmental control system

performs the cabin temperature control function where engine bleed air drives air conditioning packs that provides conditioned air to the different temperature controlled zones within an aircraft's cabin.

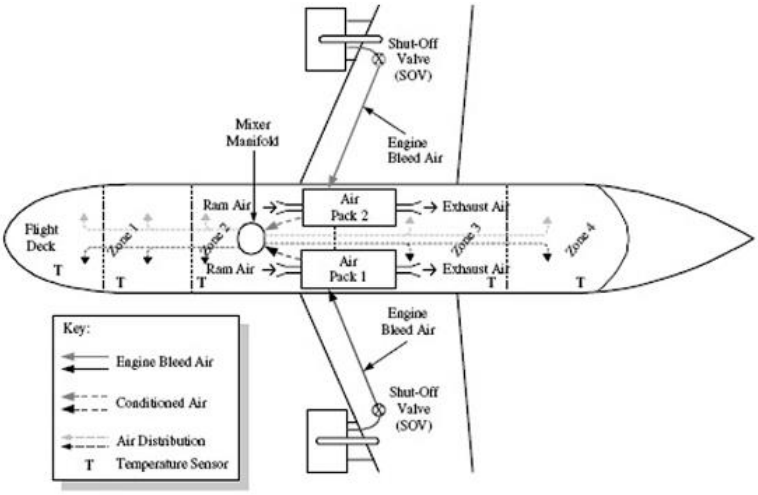

Figure 4: Cabin temperature control system example [11].

This research assumes that the environmental control system is driven by an air cycle machine. Air cycle machines cool engine bleed air down to temperatures that are sustainable within the cabin environment for aircraft occupants. The basic principle for air cycle machines is that energy is removed by a heat exchanger from compressed air which then performs work by passing through a turbine which drives the compressor, and hence the energy is transferred resulting in a reduction in temperature and pressure [11].

Aircraft ice protection systems are responsible for protecting aircraft wings (and other critical components not considered for this research such as nacelles and stabilizers) from ice and ensure aircraft maneuverability in icing conditions. Wing ice protection systems keep ice from accumulating on the wing leading edge, therefore preventing the degradation of aerodynamic performance. This function is performed by heating the skin of the wing leading edge; this research further elaborates that heating is performed by exchanging heat with hot bleed air

provided by the aircraft pneumatic system through piccolo tubes. A schematic showing a typical wing ice protection system and the flow of hot air within a wing's leading edge is shown in Figure 5.

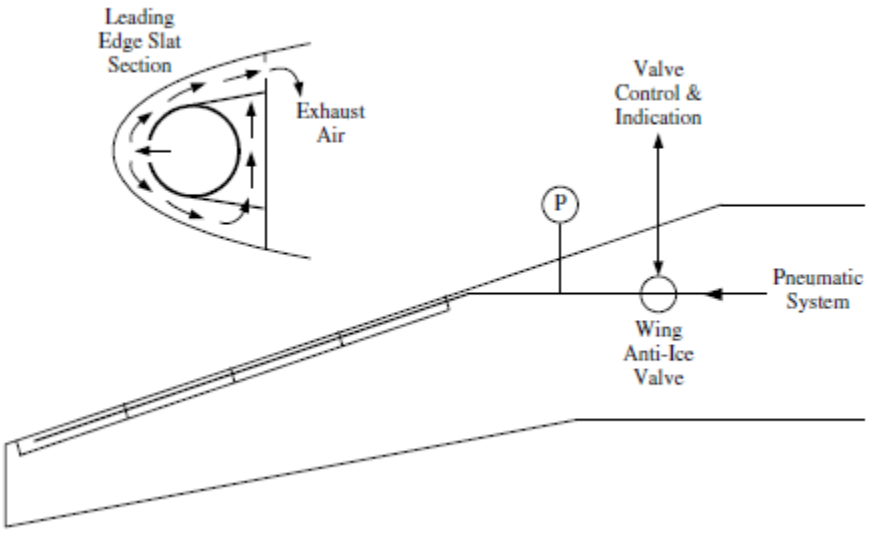

Figure 5: Typical wing ice protection system [11].

3.2 Environmental Control System Model

Environmental control system design uses an integrated approach where the air cycle machine is responsible to perform multiple functions of the systems. In order to model the behavior of the air cycle machine, it is necessary to determine the flow schedule and engine bleed characteristics. Engine bleed characteristics are driven by engine performance at each flight phase and are already modeled part of the existing MDO environment. Flow schedule is the amount of flow required to perform the system functions at every flight altitude. The flow schedule is dependent mainly on aircraft heat loads, ventilation requirements, aircraft leakage and depressurization requirements. Figure 6 shows a flowchart of the analysis required to model the performance of an air cycle machine.

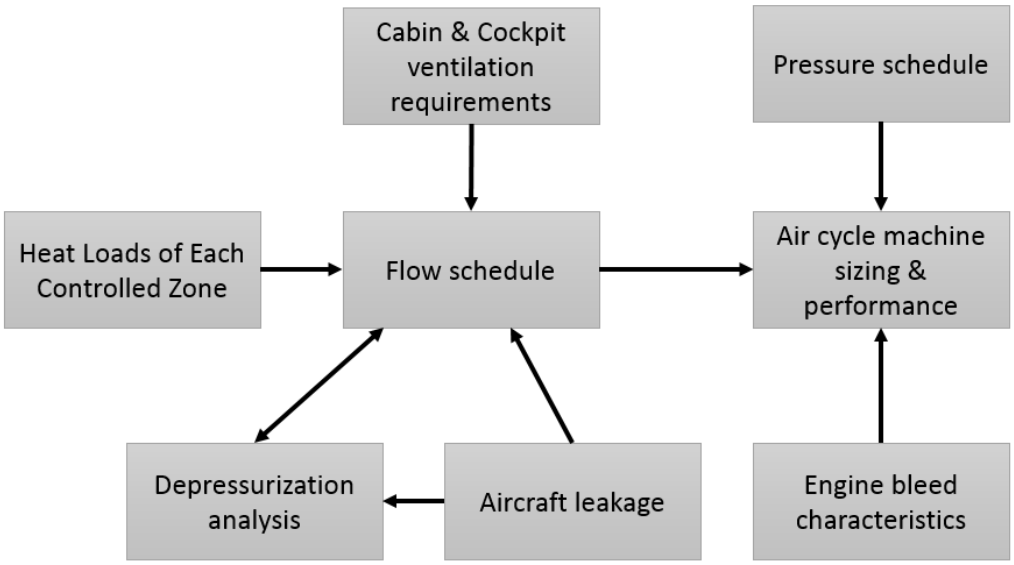

Figure 6: Environmental control system top level design flow chart.

This section describes the methodology used to model all the components needed to predict the behavior of the environmental control system due to changes to environmental conditions, aircraft top level parameters, and to engine bleed characteristics.

3.2.1 Heat Loads Calculation

Each aircraft zone is considered to have its specific heat loads that shall be cooled by the air conditioning system across all phases of flight. Heat loads are a combination of the following loads:

- External heat loads
- Metabolic heat loads
- Solar heat loads
- Electrical heat loads

In this section, a description of the methodology behind every type is described. The total heat loads for every temperature controlled zone is the addition of each type of heat load in each specified flight phase.

External Heat Loads

These are the loads that are due to the conduction between the skin of the aircraft and the studied zone. These loads are calculated for each controlled temperature zone as per [14]

$$HL_{Ext} = UA_{sk} \times (T_{zone} - T_{skin}), \quad (1)$$

where HL_{Ext} denote external heat loads, UA_{sk} is the thermal conductivity of the aircraft skin, T_{zone} is the temperature in the considered zone (cabin or cockpit), and T_{skin} is the aircraft skin temperature.

Several linear correlations were developed to calculate the UA based on the wetted area of the outer skin of the desired zone.

The temperature zone is supplied from the aircraft level requirements and is assumed to be 24°C. The aircraft skin temperature can be determined as per [14]

$$T_{skin} = T_{ambient} \times (1 + 0.18 \times M^2), \quad (2)$$

where $T_{ambient}$ is the ambient temperature and M is the flight Mach number; these are determined based on the mission identified by the aircraft performance model already existing in the MDO environment.

The Mach number and the ambient temperature are determined based on the mission identified by the aircraft performance model already existing in the MDO environment.

Metabolic Heat Loads

The metabolic heat load is based on the number of passengers and crew during the desired flight type and is calculated using Eqs. (3) and (4), as per [14].

$$HL_{Pax} = N_{pax} \times (188 - 4.7 \times T_{cabin}) \quad (3)$$

$$HL_{Crew} = 2 \times N_{crew} \times \left(188 - 4.7 \times T_{cockpit}\right), \quad (4)$$

where HL_{Pax} denote passenger heat loads, HL_{Crew} denote crew heat loads, N_{pax} is the number of passengers, N_{crew} is the number of crew members, T_{cabin} is the cabin target temperature, and $T_{cockpit}$is the cockpit target temperature.

Solar Heat Loads

The solar heat loads for each zone can be calculated based on the effective window area of the section and the solar flux at the flight altitude. Solar heat loads on aircraft skin is neglected assuming that a typical aircraft will be painted white. The equation to calculate solar heat loads is as per [14]

$$HL_{solar} = (S_{windows} + S_{windshield}) \times \varphi \, , \quad (5)$$

where HL_{solar} denote solar heat loads, $S_{windows}$ is the cabin window area, $S_{windshield}$ is the cockpit windshield area, and ϕ is the solar flux looked up based on the data depicted in Figure 7.

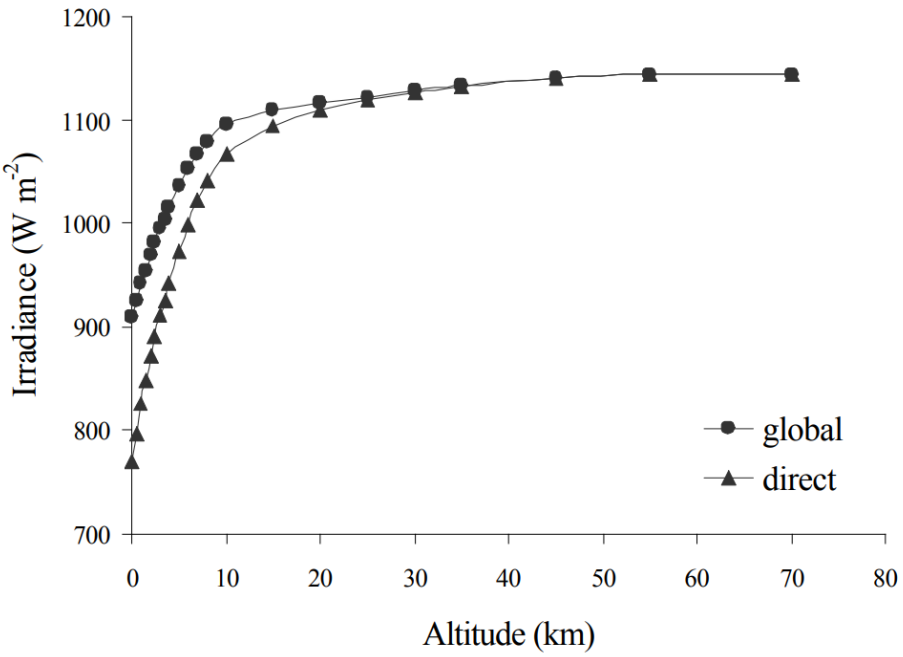

Figure 7: Solar flux (irradiance) versus altitude [15]

Electric Heat Loads

These loads depends on the electric equipment installed in each zone and is a fixed number for each type of demand (cooling or heating) and for every aircraft zone. Electric heat loads are comprised of the following:

- Interior lighting systems
- Cabin management systems
- Cabin entertainment systems
- Galley equipment (oven, chiller, coffee machine)
- Cockpit display and electronic equipment
- Avionics racks within the cabin or the cockpit

In terms of electrical heat loads of the cabin, a correlation was developed between lighting heat loads and cabin length. A detailed list of cabin systems and appliances with rated power usage should be provided for every aircraft type to be studied. Cockpit electrical heat loads are also aircraft specific and should be provided for every aircraft type.

Avionics racks installed in the cabin reject some heat into the zone they are installed in. The heat load from these racks is scaled based on the visible surface area of the rack inside the cabin and the equipment installed in the racks. Avionics bays installed in the under floor are assumed to not reject heat into the cabin nor cockpit zones.

3.2.2 Flow Schedule Determination

As shown in Figure 6, the flow schedule of air supplied to the cabin is dependent on several aspects such as heat loads, aircraft leakage, aircraft ventilation, and aircraft depressurization. The approach used for this research is to calculate the required flow rate for each flight phase and environmental condition based on cabin and cockpit heat loads. The flow schedule is then checked against ventilation, leakage, and depressurization analysis results to ensure the flow is adequate.

The required flow to achieve the target temperature for the cabin is determined by considering the total heat loads in the cabin and the difference between the target cabin temperature and the cabin ECS distribution temperature.

$$Q = \dot{m} \times C_p \times \Delta T \ , \tag{6}$$

where Q is the cabin or cockpit heat load, $\dot{m}$ is the air mass flow rate, C_p is the air specific heat, and ΔT is the temperature difference between air supply and zonal temperature.

The cabin distribution temperature is based on a fixed ΔT after the trim air input to the mix manifold outlet temperature. The same procedure is used to determine the required cockpit flow. Note that for this research, heat losses due to distribution ducts are not considered.

The flow split between the cabin and the cockpit is assumed to be sized from a hot day case on ground where the pack is assumed to be balanced with no trim air needed.

The total flow to cool the cabin and cockpit is then the sum of the two flows found for each zone. This flow can come from the air cycle machine only or it can be a mix of recirculation and fresh flow. It is assumed that no recirculation system is used however the capability to add a recirculation system is included in the developed model.

The methodology used is to calculate the flow split from ground cases and then determine the amount of trim air required to reach the target temperature in other flight conditions. The sizing condition for flight is a cold day since the cabin heats losses are more significant. Therefore after determining the ground flow rate and the flow split between the cabin and the cockpit, the cold day flow rate is calculated using the following assumptions:

- The air cycle machine discharge maximum temperature is set using the cockpit zone assuming that the cockpit has lower heat loads than the cabin. This is used later on in the air cycle machine model.
- A constraint for the cabin duct inlet flow temperature of a maximum 70°C which fixes the duct outlet temperature because of the ΔT loss along the duct.

After calculating the flow rate on ground and in flight, a flow schedule can be generated based on the assumption that the air mass flow rate varies linearly between ground and aircraft ceiling as shown in the sample flow schedule shown in Figure 8.

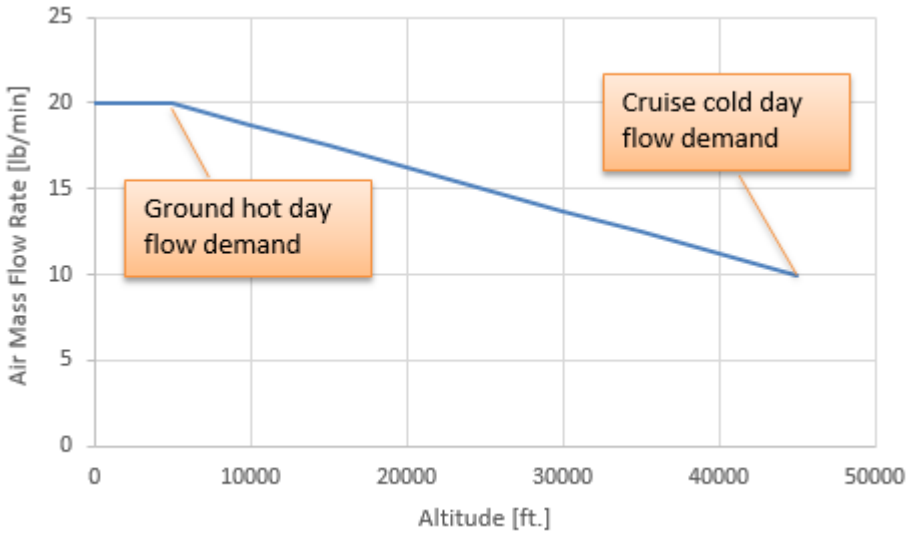

Figure 8: Sample flow schedule versus altitude

3.2.3 Aircraft Ventilation Requirements

Air is composed principally of 78 percent nitrogen and 21 percent oxygen. As altitude increases, the total quantity of all the atmospheric gases reduces rapidly, as shown for the case of oxygen in Table 1. And a reduction in the normal oxygen supply alters the human condition. It causes important changes in body functions, thought processes, and the maintainable degree of consciousness. The resultant sluggish condition of mind and body produced by insufficient oxygen is called hypoxia [22].

Table 1: Oxygen pressure in the atmosphere at various altitudes [22].

Altitude MSL (feet)	Oxygen pressure (psi)
0	3.08
5,000	2.57
10,000	2.12
15,000	1.74
20,000	1.42
25,000	1.15
30,000	0.92
35,000	0.76
40,000	0.57

Aircraft certification authorities therefore created requirements to prevent aircraft occupant hypoxia due to oxygen deficiency in the form of minimum fresh air mass flow rate. As per the Federal Aviation Regulations section 25.831 (a), "*...For normal operating conditions, the ventilation system must be designed to provide each occupant with an airflow containing at least 0.55 pounds of fresh air per minute*."

Fresh air is air that is taken from the ambient environment. For the case of a pneumatically powered environmental control system, fresh air is the bleed air taken from engine bleed ports and supplied to the cabin through an air cycle machine. For ambient and heat load conditions that are less severe than the design cases, the minimum flow that the air cycle machine provides must satisfy passenger ventilation requirement and must maintain cabin pressure.

3.2.4 Aircraft Air Leakage Estimation

Air leakage during aircraft pressurization can be caused due to gaps in structures joining, installation of components, windows, doors, windshields etc. Air leakage must be taken into consideration when analyzing passenger ventilation requirements and for aircraft depressurization analysis. A simplified method was used to predict aircraft leakage depending on

cabin and cockpit wetted area as shown in Figure 9. The data shown in Figure 9 are known from existing aircraft.

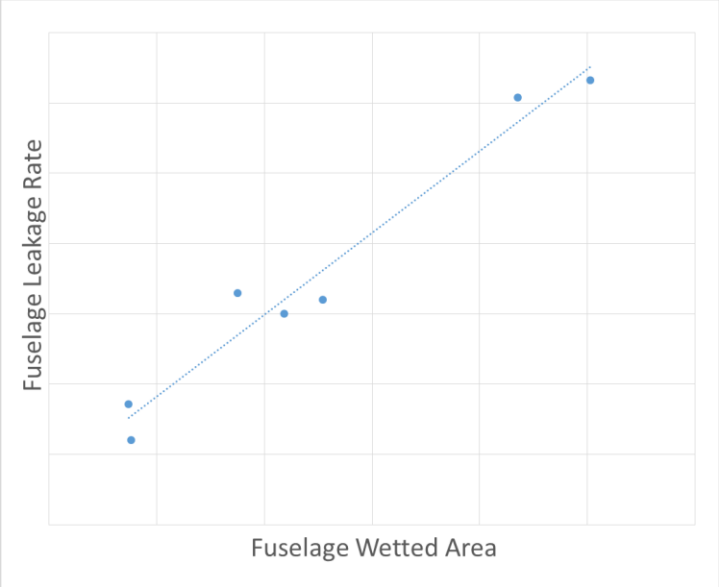

Figure 9: Fuselage air leakage rate correlation using existing aircraft test data

The air leakage flow rate is then converted to an effective leakage area at aircraft end of life. The scaling method is studied at fixed flight and environmental conditions. Therefore, the leakage flow is scaled using the effective leakage area for different flight conditions in the environmental control system model.

3.2.5 Depressurization Analysis

Aircraft depressurization happens due to a crack that developed in the pressurized zone. After a depressurization, cabin altitude (which is a term used to describe cabin pressure) starts dropping, so the aircraft's pilot performs a maneuver called emergency descent to ensure cabin altitude does reach non-survivable conditions. The Federal Aviation Regulations as per 25.841(a) dictate that "*…(2) The airplane must be designed so that occupants will not be exposed to a cabin*

pressure altitude that exceeds the following after decompression from any failure condition not shown to be extremely improbable:

(i) Twenty-five thousand (25,000) feet for more than 2 minutes; or

(ii) Forty thousand (40,000) feet for any duration."

Therefore after an emergency decent, a requirement was set for cabin altitude not to reach an altitude of 25000 ft. for more than 2 minutes. Aircraft altitude profile in an emergency descent is dependent on wing configuration and the spoiler system design [2]. An example analysis of a cabin depressurization followed by an emergency descent is shown in Figure 10.

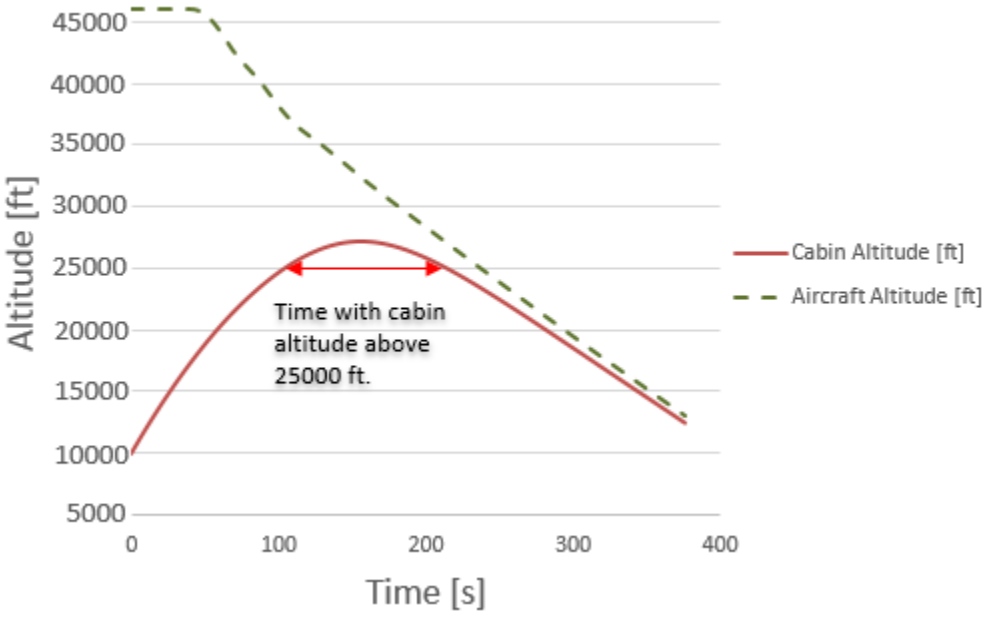

Figure 10: Example of a depressurization analysis studying aircraft and cabin pressure.

3.2.6 Air Cycle Machine Model

The air cycle machine (ACM) was modeled adopting the approach reported in [21], and was verified to produce the same simulated results. The architecture assumed for the ACM in the

environmental control system model is shown in Figure 11. The heat loads used downstream of the ACM are calculated based on 3.2.1 while the bleed characteristics are calculated by the engine model based on flight conditions and engine bleed port characteristics.

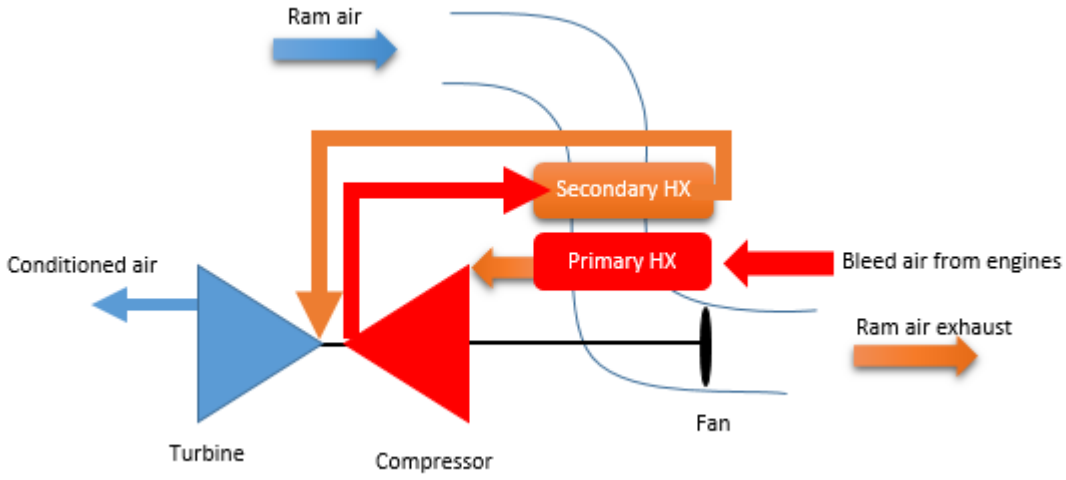

Figure 11: Architecture of a typical air cycle machine

The developed model can predict the impact of changes in bleed conditions on the output of an ACM and was used as a constraint in the aircraft MDO problem where the cooling power available at any flight condition should be equal to or higher than the specified heat loads. The model is based on a methodology discussed in [21]. The thermodynamic model of the considered air cycle machine can be described in the temperature versus entropy graph shown in Figure 12.

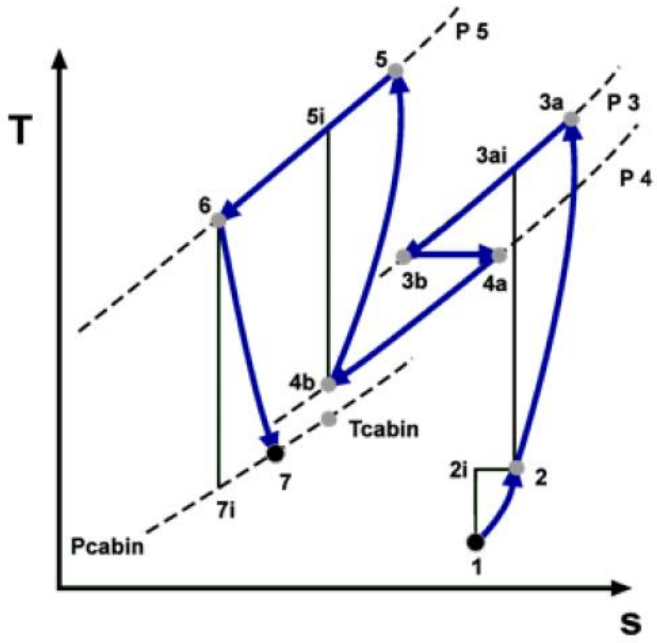

Figure 12: Temperature versus entropy diagram of an aircraft air cycle machine [21].

3.3 Wing Ice Protection System Model

This section describes the methodology used to model the bleed demand required for ice protection systems starting by predicting ice catch of a wing, then estimating the power required to protect the wing from icing, and finally calculating the bleed air requirements to provide the thermal energy needed for ice protection.

3.3.1 Ice Catch Rate Prediction

Ice catch rate, or water catch rate, is the ratio of ice accumulated on an aircraft's wing as it flies relative to the water content it experiences in icing conditions. Ice accretion on wing may cause aerodynamic performance degradation and control and maneuverability issues. Several analysis methods have been developed to predict ice catch and ice shapes ranging from low fidelity to

high fidelity methods [22], [29]-[32]. An example validation of ice catch and shape prediction methods is shown in Figure 13.

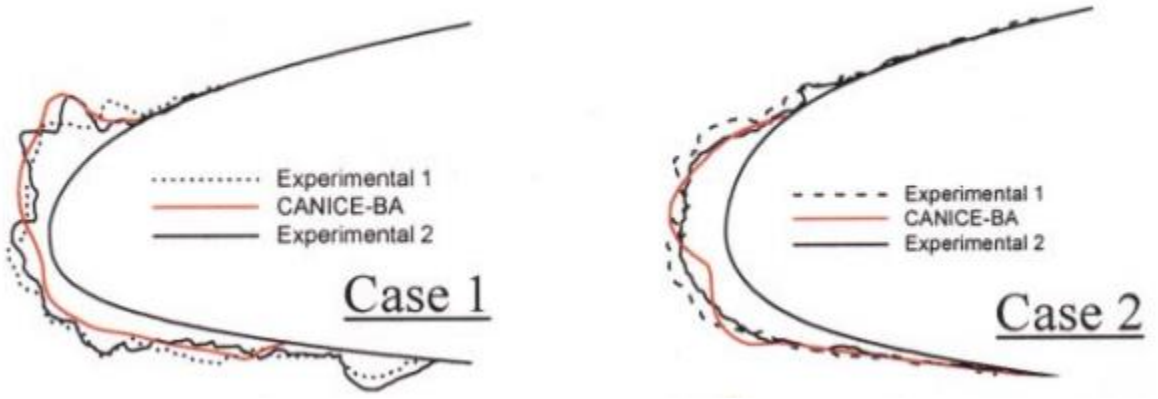

Figure 13: Comparison of a high fidelity ice shape prediction method (CANICE-BA) with experimental results (Experimental 1, 2) [29]

For the purposes of this research, a low fidelity prediction model was sufficient since it is used as a proof of concept of the integration of the overall models into one environment. A simplified model was created to predict the ice catch rate of a wing with the possibility to input a catch rate in case higher fidelity data exists. The simplified model is based on an analytical approach as per [22]. The method was validated and proven to provide good correlation with catch rates calculated from wind tunnel data.

The fundamental equation for total water catch is

$$M = 0.8vB(LWC)E_m \tag{7}$$

where, v: airspeed, B: airfoil maximum thickness, LWC: liquid water content, E_m: total water catch efficiency, M: Total water catch per ft of span.

For a given volume median droplet size, ambient temperature, and altitude, water catch efficiency, E_m is a function of velocity, airfoil shape, and thickness. Reference [22] shows

several methods for estimating E_m. For the purposes of this study, the value of E_m was calculated and fixed for the 2 test cases that will be described in Section 5.2 since the variables affecting E_m are within the tolerances range described in [22]. LWC , which is the amount of super-cooled water contained in an icing cloud, was also assumed to be fixed since only one icing flight phase is studied for this research as described in section 4.2.

3.3.2 Ice Protection Power Requirement Model

After estimating the ice catch rate, the power requirements to protect the wing can be calculated. First the external heat transfer coefficient needs to be calculated to find the external film conductance. The method chosen to estimate the external film conductance is adapted from [22] and is described in

$$C_o = 6.32[(\rho g)_o v L_x] \tag{8}$$

where, v: airspeed ,$(\rho g)_o$: ambient air density, L_x : length of protected surface, C_o : external film conductance per ft of span of protected surface.

Several methods exist to protect an aircraft's wing from icing. The two methods assumed for this research are fully evaporative anti-icing and running wet anti-icing. Fully evaporative anti-icing, as the name suggests, fully evaporates all water impinging on an aircraft wing's protected section. Running wet anti-icing allows some of the imping water to run back and freeze aft of the protected area on the leading edge of a wing. In this research, a mix between the 2 methods is assumed where the top surface of the wing's leading edge is protected using the fully evaporative method, and the bottom surface is protected using the running wet method.

As described in [22], the requirements of a hot air evaporative anti-icing system are determined by the rate at which heat must be supplied to balance the heat losses from the protected surface,

which result from three concurrent processes: convective cooling, evaporation, and sensible heating (heating of the impinging water to the skin temperature).

The heat load equation for fully evaporative anti-icing (adapted from [22]) is shown in Eq. (9).

$$\frac{q}{C_o} = T_{sk} - T_{aw} + \left[\frac{M}{C_o} * (T_{sk} - T_w)\right] + \left(\frac{M}{C_o} * L_e\right) \tag{9}$$

$\overleftrightarrow{\text{Convective heat}}$ $\overleftrightarrow{\text{Sensible heat}}$ $\overleftrightarrow{\text{evaporation}}$

The heat load equation for running wet anti-icing (adapted from [22]) is shown in Eq. (10).

$$\frac{q}{C_o} = T_{sk} - T_{aw} + \left[\frac{M}{C_o} * (T_{sk} - T_w)\right] + \left(\frac{2.9 L_e (p_{sk} - p_w)}{P_{amb} - p_{sk}}\right), \tag{10}$$

$\overleftrightarrow{\text{Convective heat}}$ $\overleftrightarrow{\text{Sensible heat}}$ $\overleftrightarrow{\text{evaporation}}$

where q is the heat flow, C_o is the external film conductance per ft of span of protected surface, T_{sk} is the wing skin temperature, T_w is the total temperature of atmospheric water, T_{aw} is the adiabatic wall temperature, L_e is the latent heat of evaporation, P_{amb} is the ambient static pressure, p_{sk} is the saturation pressure of water vapor at T_{sk}, and p_w is the saturation pressure of water vapor at T_w.

This method is modeled at several sections of the wing. Then the total power demand of the sections is added to calculate the bleed demand of the whole wing ice protection system.

3.3.3 WIPS Bleed Demand Calculation

The bleed flow demand calculation is based on the power requirement assessment. The following assumptions used to within the model:

- A closed loop temperature controlled system is considered therefore no additional bleed is required for contingency.
- Pre-cooled bleed air temperature of 232°C with a fixed drop in temperature in the pneumatic system is used as an input to the WIPS.
- The holding flight case in icing condition at a fixed aircraft speed is assumed to be the worst case and would be the driving factor for engine bleed demand.
- The upper section of the leading edge uses a fully evaporative ice protection scheme.
- The lower section of the leading edge uses a running wet ice protection scheme.
- Single leading edge skin within the protected section used to derive the energy efficiency.

The flow required for every section is calculated using

$$\dot{m}_{WIPS} = \frac{q}{\varepsilon_{sk} C_p (T_{WIPS} - T_{sk})}, \tag{11}$$

where $\dot{m}_{WIPS}$ is the WIPS mass flow rate requirement, q is the heat flow requirement, ε_{sk} is the thermal efficiency of protected skin, and T_{WIPS} is the temperature of bleed air within the ice protection system.

The calculated flow for all the sections is then summed to calculate the total flow requirement for WIPS which is used for pneumatic system and precooler sizing.

3.4 Pneumatic System Model

The pneumatic system as shown in the sample architecture drawing in Figure 3 is responsible to deliver air between consumers and producers of pressurized bleed air. Pneumatic systems also

feature a precooler to lower bleed air temperature to comply with FAR Advisory Circular 25.981-1C as per the following requirement:

"…The auto-ignition temperature of fuels will vary because of a variety of factors (ambient pressure, dwell time, fuel type, etc.). The value accepted by the FAA without further substantiation for kerosene fuels, such as Jet A, under static sea level conditions, is 450 °F (232.2 °C). This results in a maximum allowable surface temperature of 400 °F (204.4 °C) for an affected component surface."

Therefore, a precooler limits bleed air temperature up to a maximum of 232.2 °C to prevent any fuel tanks from reaching the maximum allowable temperature for ignition prevention. A precooler is typically a heat exchanger that uses engine fan air or ambient ram air as the cold flow stream and engine bleed air as the hot flow stream. A model to size and calculate the performance of a precooler was developed.

The precooler sizing model first estimates the enthalpy for heat dissipation within the precooler using the following equation (adapted from [14])

$$P_{PCE,diss} = C_p \times \dot{m}_{hot\ side} \times \left(T_{bleed} - T_{regulated}\right), \quad (12)$$

where, $P_{PCE,diss}$: heat dissipated through the precooler , C_p : specific heat capacity of air, $\dot{m}_{hot\ side}$: hot side mass flow rate, T_{bleed} : bleed temperature, $T_{regulated}$: regulated bleed temperature by precooler.

The maximum hot side flow rate is conservatively assumed to be the addition of ECS ground flow rate and the WIPS holding flow rate. A correlation was created between precooler size and power dissipated through the precooler at maximum hot side flow.

The other major components for the pneumatic system are the high pressure (HP) ducting and valves. For the purposes of this research HP ducting pressure losses are assumed to be fixed. The weight of HP ducting and valves are modeled and estimated as described in 3.6.

3.5 Systems Drag Prediction Models

As will be discussed in section 4.2, the parameters that impact drag caused by air systems in the aircraft MDO setup are the precooler and the ram air inlet/outlet for the ACM heat exchangers. These parameters are a function of the ECS flow rate and the WIPS flow rate. Drag impact due to air systems is estimated for the cruise phase by studying several points of the variables mentioned above and creating a simplified method as follows

$$P_{PCE,diss} = C_p \times \dot{m}_{hot\ side} \times \left(T_{bleed} - T_{regulated}\right), \tag{13}$$

where, $C_{d,air}$: additional drag counts due to air systems, $K_{d,RAM}$: factor for drag cause by RAM air, $\dot{m}_{RAM}$: ram air mass flow rate during cruise, $K_{d,PCE}$: factor for drag caused by precooler exhaust, $\dot{m}_{PCE}$:total mass flow rate passing through precooler including hot and cold sides.

3.6 Systems Weight Prediction Models

For the purposes of this study, impacts on weight have been limited to wing ice protection systems and to the pneumatic system. The environmental control system is assumed to be fixed for a certain aircraft configuration where the changes in aircraft parameters do not necessitate a major change in the ACM design.

The pneumatic system weight impact is due to changes in the precooler size and the HP ducting which are calculated using correlations similar to the drag prediction correlation used in 3.5.

4. MDO INTEGRATION

4.1 Aircraft MDO Environment

The developed models were integrated in an existing monolithic MDF architecture as shown in Figure 14. The objective of the MDO problem is to minimize the maximum take-off weight of the aircraft while satisfying certain constraints, which, prior to the consideration of air systems, include:

- Performance requirements
- Stability and control requirements
- Landing gear integration
- Flight control system integration

Aircraft performance requirements are discussed in detail in [2] and [4], and include requirements for cruise speed and altitude, initial cruise altitude, approach speed, balanced field length, etc.

Landing gear integration constraints discussed in detail in [12] and [13], and include geometrical constraints such as kinematics of retractions of the main landing gear, in addition to ground handling constraints such as tip over and turnover requirements.

Stability and control requirements include

Flight control system integration constraints are geometrical constraints that include a minimum wing thickness at specific span and chord locations to reserve space for flight control actuators.

The design optimization variables include:

- Wing design variables (area, aspect ratio, sweep, taper ratio, thickness)

- Engine design variables (engine scaling ratio)

The definitions of wing and engine design variables along with their impact on aircraft performance is discussed in [2] and [4].

The linking variables include:

- Subsystems weight (engine, aircraft systems, structures, wing, etc.)
- Engine characteristics (including bleed characteristics, fuel consumption, etc.)
- Wing planform
- Aircraft structures (wing spars, fuel tank volume) & aero-elasticity (static and dynamic)
- Tail size and planform
- Aerodynamics parameters (drag, buffet, high speed aerodynamics, maximum lift coefficient, etc.)
- High lift system parameters (flaps/slats chords and deflection)

Note that design variables are variables that are adjusted by the algorithm to minimize the objective function whereas linking variables are calculated based on design variables and exchanged between the different models/disciplines.

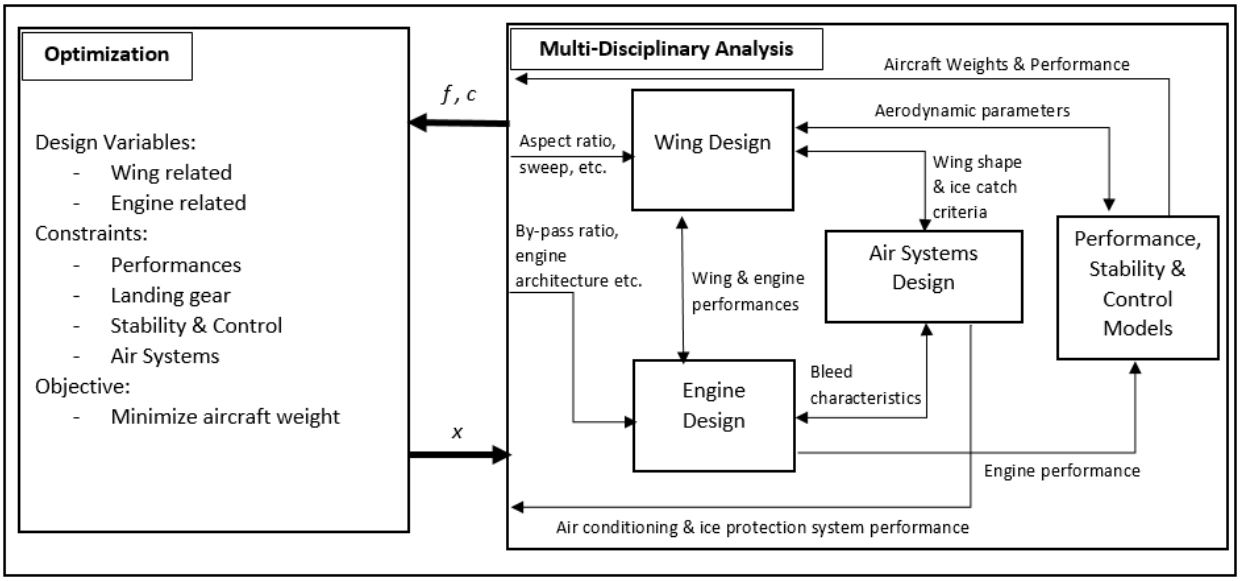

Figure 14: Schematic showing the interaction of air systems with other disciplines within the aircraft MDO problem.

The existing MDO formulation used a sequential approach for different disciplines where the optimizer calls each discipline in a sequence of models predefined. The air systems models were built using Dynamic JavaScript code in the Isight environment and integrated before the weight and balance module as shown in Figure 15.

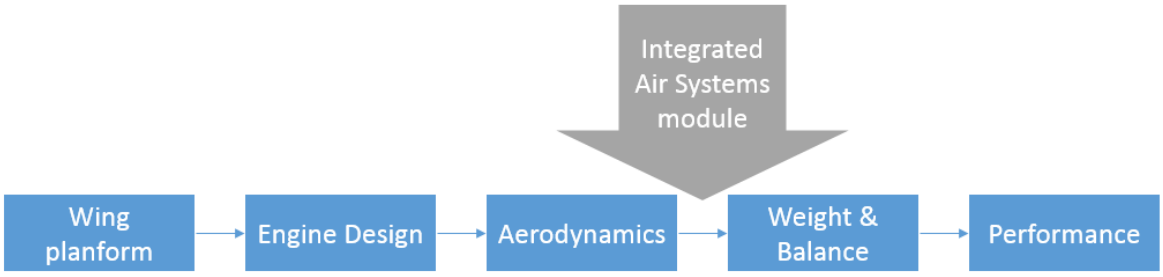

Figure 15: Sequence of modules within the existing MDO environment showing the chosen sequence for the developed air systems module

4.2 Integrated Engine-Air Systems Model within MDO

As a first step a mind map was created to visualize the impacts and dependencies of adding air systems into the described MDO environment as shown in Figure 16. The main impacts added by air systems are listed as follows:

- Depressurization analysis constraint as described in 3.2.5. The constraint checks if certification cabin pressurization requirements are met for a given aircraft/spoiler configuration and an environmental control system air mass flow rate.
- Drag impact caused by ram air demand for air cycle machine heat exchanger and precooler exhaust and can be tracked to aircraft heat loads and engine/wing design variables as shown in Figure 16. This parameter is implemented in the aircraft performance model as a fixed delta in drag.
- Aircraft weight impact caused by changes in the pneumatic system.
- Engine fuel consumption in cruise parameter impacted by ECS flow rate and engine fan air extraction flow rate.
- Ice protection capability constraint driven by the engine bleed flow availability and the wing ice protected area that are driven by engine/wing design variables.

It was decided to add air systems parameters as constraints without adding any design variables (such as cabin pressure schedule, ACM size, icing protection method) to the existing MDO problem formulation.

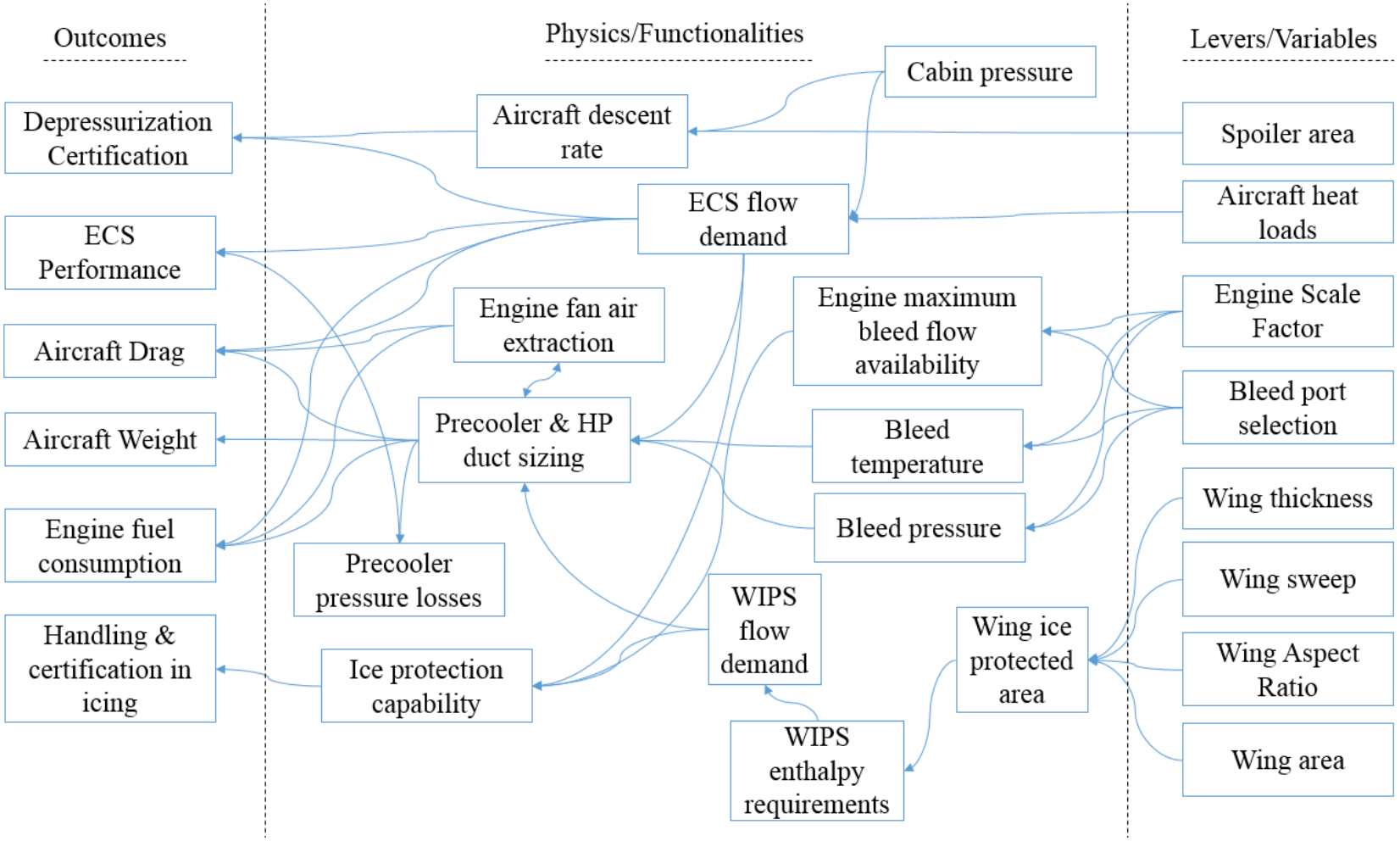

Figure 16: Mind map showing the impacts and dependencies implemented by adding air systems into the MDO environment

The integrated air systems modify the MDO problem formulation as follows:

- Additional constraints:

    1) Minimum bleed air flow rate for air conditioning per flight phase

    2) Minimum bleed air flow rate for WIPS in a holding flight under icing condition

    3) Maximum cabin exposure time of 2 minutes to altitudes above 25000 ft.

- Additional parameters:

    1) Bleed air demand parameters from ECS and WIPS

    2) Bleed air availability at each engine bleed port

    3) Engine fan air extraction

    4) Engine fuel consumption delta due to ECS bleed air demand

Possible parameters that could be considered in the future include the precooler size due to the impact on nacelle diameter therefore weight and drag.

Constraint (1) has been selected due to its impact on engine fuel consumption and consequently on aircraft performance and aircraft weight.

Constraint (2) was the only constraint selected due to WIPS due to the detrimental impact of bleed on engine in a typical holding case. This is due to the lower thrust setting in a holding flight accompanied by a high bleed demand for ice protection due to the high ice accretion at altitudes between 15,000 and 20,000 ft. Other flight phases with icing could also be investigated such as take-off, climb, and approach.

Constraint (3) was selected to demonstrate the link between aircraft performance, flight control sizing, and air system modules. As shown in Figure 16, flight spoilers sizing along with ECS flow schedule directly impact cabin depressurization and consequently cabin exposure to high altitudes.

5. ANALYSIS

5.1 Sensitivity Analyses

The first step after integrating the models into the MDO environment was to analyze the sensitivity of the objective and constraint functions to the design variables. A business jet reference transonic aircraft was used with a simple wing configuration and aft mounted engines.

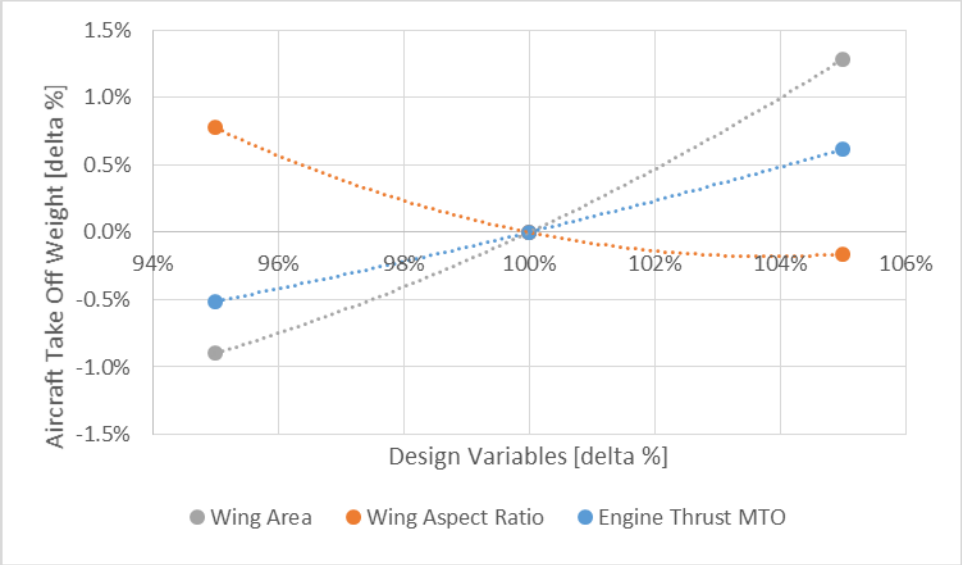

Figure 17: Sensitivity of aircraft takeoff weight

The effect of a selected set of design variables on the objective function is shown in Figure 17. Note that around the reference aircraft data point, aircraft weight is monotonically increasing with increasing wing area. An opposite trend is shown in Figure 18 where the WIPS bleed demand constraint is monotonically decreasing with increasing wing area. The WIPS bleed demand constraint is the difference between available mass flow rate of bleed supply at the engine port and the bleed demand from the WIPS in pounds per minute (ppm). It can be concluded that the sensitivity analysis is as per expectations since the WIPS bleed demand

constraint increases with an increasing engine thrust and decreases with increasing wing area and wing aspect ratio.

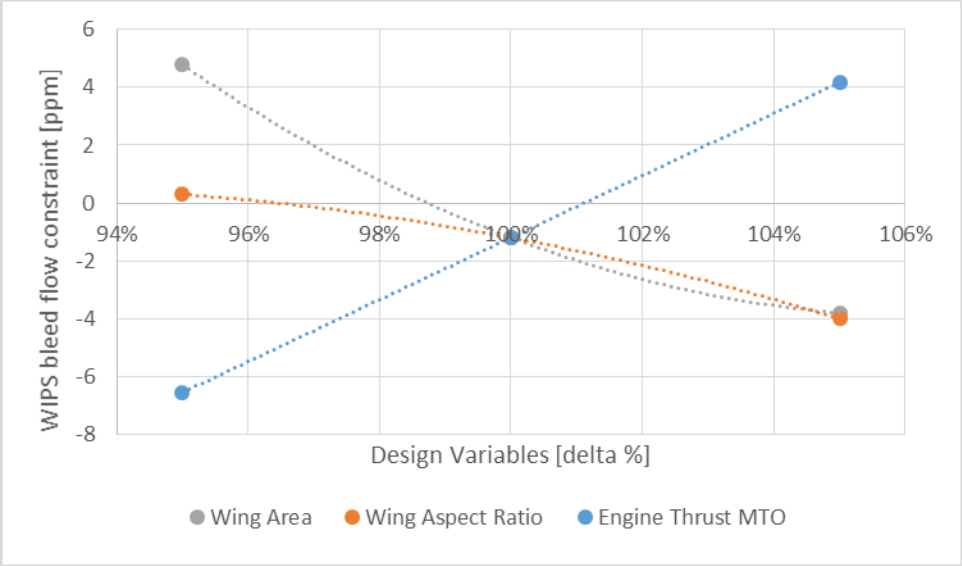

Figure 18: Sensitivity of WIPS bleed air flow rate demand in holding flight in icing conditions

5.2 Numerical Investigation

This section will report optimization results for test cases related to several reference aircraft. The reference aircraft used is a business jet aircraft with aft mounted engines and a simple wing configuration. Two test cases were identified:

- Test case 1: a fixed engine architecture and thrust with varying wing design variables
- Test case 2: a scalable engine with varying wing design variables

The two test cases were optimized with and without the developed air systems modules and the corresponding constraints.

A common starting aircraft was used for both the cases run with/without air systems. An optimization scheme was used as follows:

- Step 1: Starting from a single aircraft point an evolutionary optimization algorithm based on the built-in "Evol" optimization technique in Isight [33] evaluates a pre-defined number of alternative designs that was set to 1000.
- Step 2: An Isight built-in technique called "Pointer," which uses the design with the minimum objective function value from step 1 as a starting point, and performs a further optimization by combining a genetic algorithm, Nelder and Mead downhill simplex, sequential quadratic programming (NLPQL), and a linear solver. The details of the "Pointer" technique are unknown to the user (Isight-proprietary information).

Both test cases, and their corresponding runs, converged; the corresponding run numbers are shown in Table 4. An example of the convergence history of an aircraft optimization including air systems, test case 1, is shown in Figure 19.

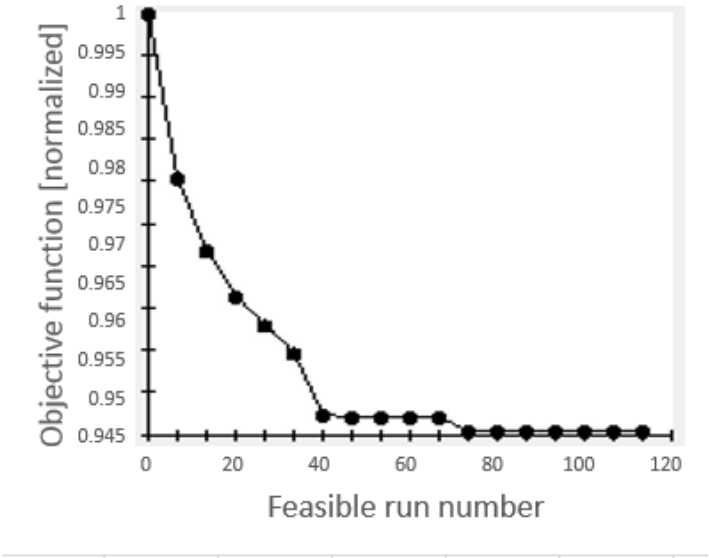

Figure 19: Convergence history of test case 1 run with air systems modules

The first test case is a sample case where engine design is fixed before aircraft design; such an approach is common for aircraft manufacturers to consider since engines are one the of long lead components that would save development time if chosen from a pre-existing platform.

A selected list of parameters from test case 1 comparing optimizations with and without air systems is shown in Table 2.

Table 2: Comparison of optimization results with and without air systems for test case 1

	Optimization without air systems constraints	**Optimization with air systems constraints**
Take-off weight (objective)	Baseline	0.2%
Block fuel (output)	Baseline	1.2%
Takeoff thrust (variable)	Baseline	0.0%
Wing span (variable)	Baseline	-3.3%
Wing area (variable)	Baseline	-4.0%

It is noted that the optimized wing planform with air systems leads to a similar aircraft maximum takeoff weight as the reference aircraft (+0.2%) with a block fuel consumption for the design mission of the aircraft (+1.2%). However, the aircraft optimized without air systems shows that the available bleed air demand for WIPS in a holding flight in icing conditions is not sufficient. The newly added air systems constraints forced the design to decrease wing area and wing span to minimize the protected area in order to meet the WIPS flow demand constraint.

A top view of the 2 optimized results of test case 1 is shown in Figure 20.

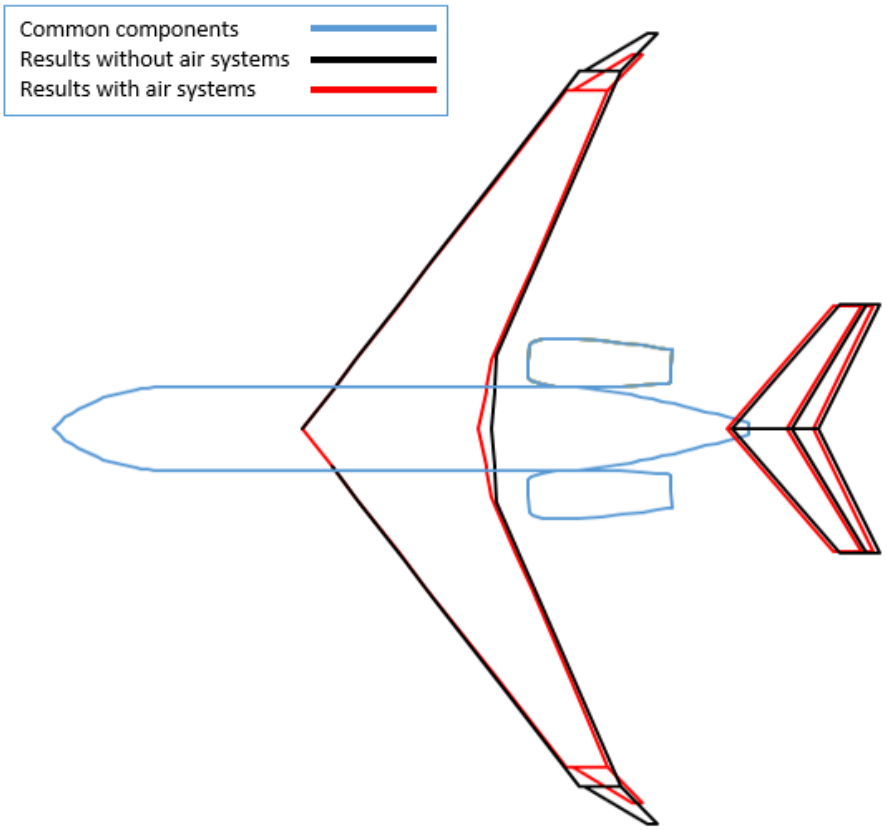

Figure 20: Comparison results of aircraft wings optimized with and without the air systems (Test case 1)

It is noted that a maximum on the sweep angle design variable was implemented. Therefore, both aircraft reach the same maximum sweep angle with a less efficient aerodynamic design in the results including air systems constraints which transforms into a higher fuel consumption over the design mission and a higher aircraft maximum take-off weight. Although this design is technically less efficient given the discussed items above, the resultant aircraft is considered more mature with less possibility of design issues arising in subsequent design stages. It should also be noted that the additional constraints added due to air systems, depressurization and ECS flow rate, were not active and did not influence the wing design directly (ECS flow rate influences the precooler size and weight and indirectly aircraft weight).

Test case 2 uses a similar aircraft configuration as test case 1 with changes to the aircraft performance requirements in addition to allowing the engine scaling factor to be a design variable. Results comparing two optimizations with and without air systems constraints is shown in Table 3.

Table 3: Comparison of optimization results with and without air systems for test case 2

	Optimization without air systems constraints	**Optimization with air systems constraints**
Take-off weight (objective)	Baseline	0.1%
Block fuel (output)	Baseline	-0.3%
Takeoff thrust (variable)	Baseline	4.6%
Wing span (variable)	Baseline	-6.6%
Wing area (variable)	Baseline	-7.1%

Similar to test case 1 results, the two optimization results in case 2 produce results with very close maximum take-off weight (0.1% difference). Although the optimization with air systems constraint is slightly heavier than the optimization without air systems, the block fuel consumption for the design mission of the former is actually less than that of the latter. This reduction in fuel consumption is partly due to the bigger engine size (4.6%) as shown in Table 3 and visually in Figure 21 which allows for a higher initial climb altitude, and consequently less fuel consumption.

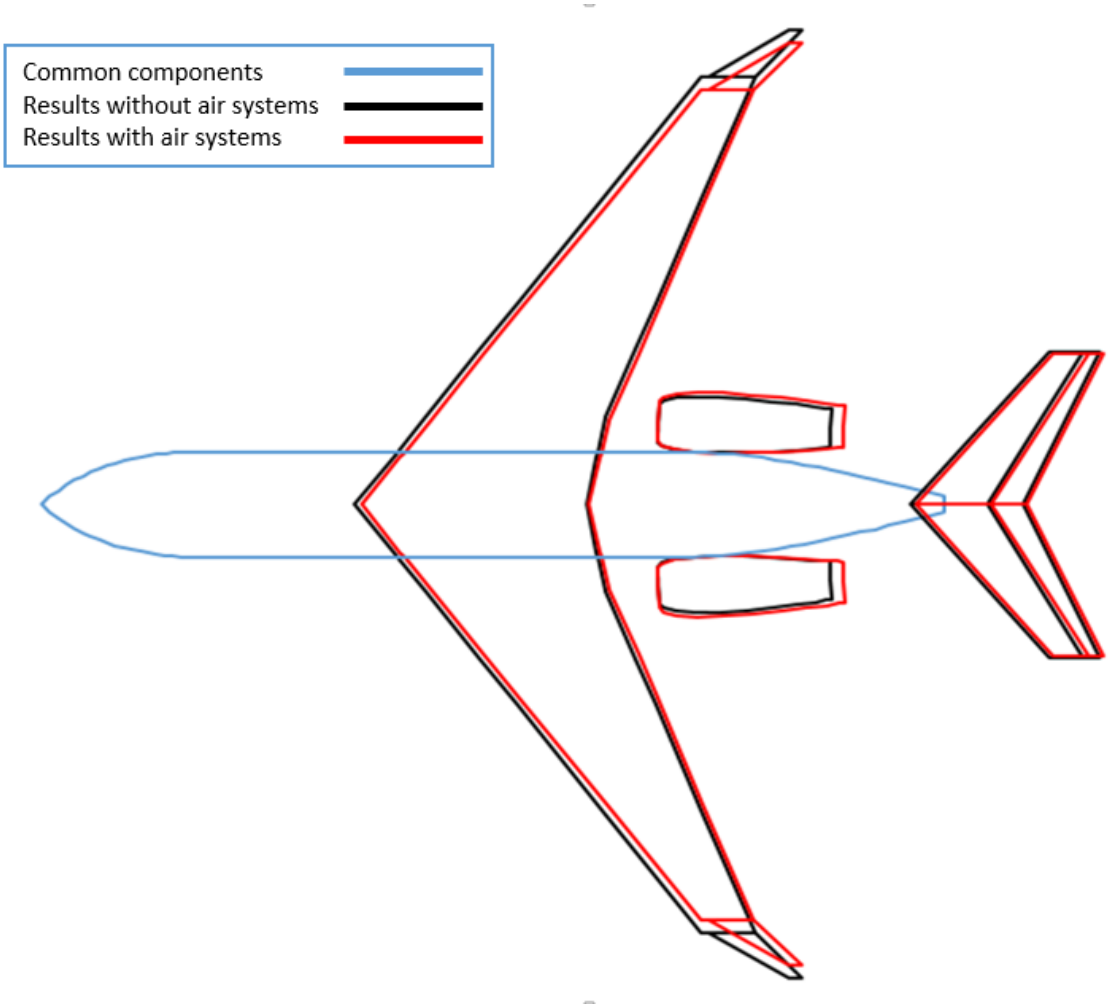

Figure 21: Comparison results of aircraft wings optimized with and without air systems considerations (Test case 2)

In addition, similar to test case 1, the available bleed air demand for WIPS in a holding flight in icing conditions is the only active air systems constraint for the results of the optimization with air systems. These results however do not negate the need to include the additional air systems disciplines and constraints. It is possible that with a different aircraft configuration, other air systems constraints could become active and drive the aircraft level design.

The detailed results of the studied test cases are shown Table 4. Design variables lower and upper bounds along with the initial values are shown. In addition, the values corresponding to the

optimal results of each test case are shown. As discussed before, the impact of adding air systems is shown in lower aspect ratio and higher taper ratio wings. Table 4 also shows the constraints used for the test cases. It is noted that the active constraints are as follows:

- Landing gear skin clearance which is a constraint for the installation of the main landing gear.
- Tip over angle which is a constraints dependent on the positioning of the main landing gear relative to the wing and aircraft center of gravity.
- Anti-icing flow constraint as discussed in the previous sections.
- Initial cruise altitude is only active for test case 2 runs where the engines have been scaled down.
- Approach speed is active on all test cases, but it is noted that test case 2 with air systems is able to meet this constraint by increasing the flap chord ratio design variable.
- Spoiler actuator clearance which is the dependent on the available space to install actuators in the wing.

Table 4: Comparison of optimization results of the two test cases

						Optimal results			
						Test Case 1		Test Case 2	
		unit	Lower bound	Upper bound	Initial value	without air systems	with air systems	without air systems	with air systems
Design Variables	Wing aspect ratio	-	6	9	7.5	7.56	7.36	7.43	7.2
	Wing area ratio	-	0.8	1.2	1	0.93	0.89	0.91	0.84
	Wing 1/4 chord sweep	degrees	25	35	30	34	35	34	35
	Wing trailing edge sweep	degrees	0	25	10	25	23	24	24
	Wing taper ratio	-	0.2	0.3	0.25	0.24	0.26	0.25	0.27
	Wing thickness factor	-	0.8	1.2	1	1.07	0.95	1.07	0.94
	Wing span ratio	-	0.8	1.2	1	0.98	0.93	0.95	0.89
	Flap chord ratio	-	0.25	0.3	0.25	0.25	0.25	0.25	0.28
	Engine scaling factor	-	0.8	1.2	1	NA	NA	0.86	0.9
Constraints	Landing gear skin clearance	inches	2	-		2.02	2.01	2.01	2.10
	Tip over angle	degrees	15	-		15.1	15.1	15.1	15.2
	Air conditioning flow constraint	ppm	0	-		10.15	9.61	9.8	9.35
	Anti-icing flow constraint	ppm	0	-		-19.78	0.09	-32.51	0.82
	Cabin exposure to high altitude	seconds	-	120		0	0	0	0
	Balanced field length	ft	-	6000		5327	5335	5890	5880
	Initial cruise altitude	ft	40000	-		43033	42580	40100	40077
	Approach speed	Knots	-	120		119.9	120	116.7	119.9
	Spoiler actuator clearance	inches	1	-		1.11	1.06	1.08	1.06
	Aileron actuator clearance	inches	0.5	-		0.71	0.65	0.64	0.61
	Number of runs	-				1822	1930	1956	2078

The impact of the studied cases above against aerodynamic coefficients is shown in Table 5 where a comparison between each aircraft's drag and lift coefficients in different flight phases is shown.

Table 5: Comparison of aerodynamic coefficients for the two test cases

		Test Case 1		Test Case 2	
		without air systems	with air systems	without air systems	with air systems
Clean	Drag coefficient	0.018	0.018	0.018	0.018
	Maximum lift coefficient	1.095	1.156	1.139	1.134
Take-off	Drag coefficient	0.044	0.044	0.044	0.044
	Maximum lift coefficient	1.623	1.694	1.676	1.677
Landing	Drag coefficient	0.087	0.088	0.087	0.088
	Maximum lift coefficient	1.902	1.976	1.958	1.961

5.3 Recommendations

Based on the results shown in the example test cases, it is evident that air systems, specifically ice protection systems, should be modeled and included in the MDO problem formulation of aircraft conceptual design. This research studied one flight phase for the ice protection system, holding in icing conditions at 16,000 ft., which typically causes issues for bleed demand. However, future changes in engine architectures and the move towards higher by-pass ratio turbofan engines could lead to more scarcity in bleed flow in other flight phases. Therefore, it is recommended to add ice protection constraints for additional flight phases such as approach and climb. The case for approach is specifically interesting given that bleed requirements for ice protection could potentially require an increase in idle thrust which would be detrimental for landing performance in cases such as steep approach.

This research was built based on an existing engine architecture using either a fixed engine or a scaled engine approach. The benefits focused on finding an optimal design while taking into consideration air system design and constraints. However, the inclusion of engine architecture and sizing as design variables would open up the possibility for a ‘true’ aircraft level optimum similar to the approach discussed in [7] and shown in Figure 22. It is recommended to study the effect of varying engine architecture and possibly bleed ports on the results of the studied MDO problems. It is expected that varying engine architecture would provide the flexibility to drive air systems parameters without the need to increase thrust, change wing planform design variables, or increase aircraft weight.

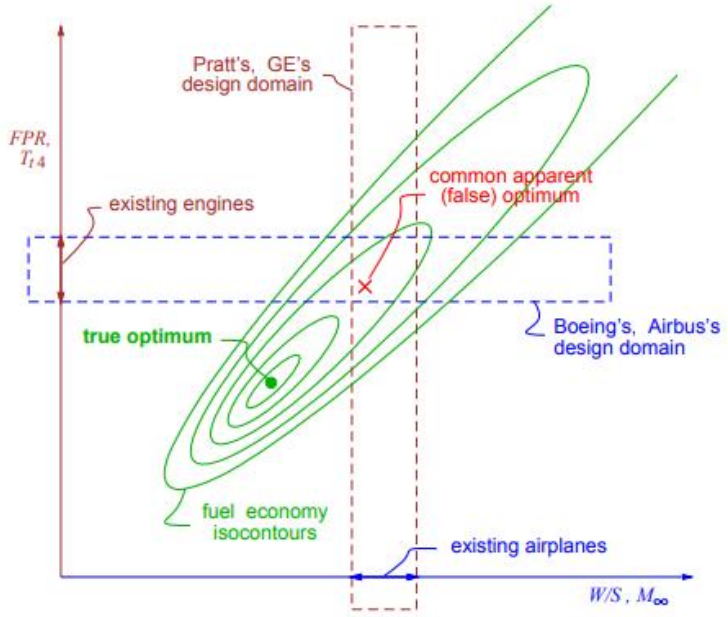

Figure 22: An example of a true optimum existing out of design space [7]

In this work, wing airfoil geometry was considered to be fixed using scalable thickness to chord ratios which was the methodology used in the existing MDO environment. Airfoil optimization is usually performed using high-fidelity optimizations with a limited number of disciplines involved such as aerodynamics, wing structures, flight controls, and landing gear. It is recommended to add a high-fidelity ice catch prediction methods into an airfoil optimization environment. The added benefit of such an approach would be to study a multi-objective optimization where minimizing ice catch in specific flight conditions can be used as part of the objective function. Results from such a methodology would ensure that ice protection capabilities are met without the need to impact aircraft engines or wing configurations.

6. CONCLUSIONS AND OUTLOOK

This research developed a methodology to model and integrate air systems into aircraft multidisciplinary design optimization for use in the conceptual design phase. The air systems modeled are the environmental control systems, wing ice protection system, and the pneumatic system. The developed physics-based models were integrated into an existing MDO environment.

Two cases of business jets with simple wing configurations and aft mounted engines were identified. The cases were optimized with and without the developed air systems models as part of the MDO analysis. In both cases, aircraft design was impacted due to the additional constraints brought about by the air systems modules with minimal change on the overall objective function. The driving case for both test cases was the wing ice protection capability by the engine. The test cases showed the importance of including air systems design in aircraft conceptual design and aircraft multidisciplinary design optimization.

REFERENCES

[1] Phillips, Rachel, Kevin Neailey, and Trevor Broughton. "A comparative study of six stage-gate approaches to product development." Integrated Manufacturing Systems 10.5 (1999): 289-297.

[2] Roskam, J., Airplane Design, Roskam Aviation & Engineering Corp., Ottawa, Kansas, 1985

[3] Mooney, D., BOEING 787–8 Design, Certification, and Manufacturing Systems Review, 2014.

[4] Sadraey, Mohammad H. Aircraft design: A systems engineering approach. John Wiley & Sons, 2012.

[5] Kesseler, E., and Guenov, M., "Advances in Collaborative Civil Aeronautical Multidisciplinary Design Optimization", Progress in Astronautics and Aeronautics, 233 Published by AIAA, © 2010, ISBN-10: 1-60086-725-1; ISBN-13: 978-1-60086-725-5.

[6] Holden C., Burden A., Bressloff W., Keane A.K., "Method of Design Optimisation", Airbus UK Limited, United States Patent 2010/0318327 A1, December 2010.

[7] Drela, M., "Simultaneous Optimization of the Airframe, Powerplant, and Operation of Transport Aircraft", MIT Department of Aeronautics and Astronautics Cambridge, Massachusetts, USA, 2010.

[8] Piperni, P., Deblois, A., and Henderson, R., "Development of a Multilevel Multidisciplinary-Optimization Capability for an Industrial Environment," AIAA Journal, vol. 51, 2013, pp. 2335–2352.

[9] Raymer, Daniel. Enhancing aircraft conceptual design using multidisciplinary optimization. Diss. Institutionen för flygteknik, 2002.

[10] Yuhas, A., and Ray, R., "Effects of bleed air extraction of thrust levels on the F404-GE-400 turbofan engine," 28th Joint Propulsion Conference and Exhibit, Jun. 1992.

[11] Moir, I., and Seabridge, A., "Aircraft Systems: Mechanical, Electrical, and Avionics Subsystems Integration, Third Edition," 2008.

[12] Chai, Sonny, and William Mason. "Landing gear integration in aircraft conceptual design." 6th Symposium on Multidisciplinary Analysis and Optimization. 1996.

[13] Tfaily, Ali, et al. Landing Gear Integration in an Industrial Multi-Disciplinary Optimization Environment. No. 2013-01-2319. SAE Technical Paper, 2013.

[14] Liscouet-Hanke, Susan. A model-based methodology for integrated preliminary sizing and analysis of aircraft power system architectures. Diss. Institut National des Sciences Appliquées de Toulouse, 2008..

[15] Oumbe, Armel, and Lucien Wald. "A parameterisation of vertical profile of solar irradiance for correcting solar fluxes for changes in terrain elevation." Earth Observation and Water Cycle Science Conference. ESA, 2009.

[16] Bodie, M., Russell, G., Mccarthy, K., Lucas, E., Zumberge, J., and Wolff, M., "Thermal Analysis of an Integrated Aircraft Model," 48th AIAA Aerospace Sciences Meeting Including the New Horizons Forum and Aerospace Exposition, Apr. 2010.

[17] Pérez-Grande, Isabel, and Teresa J. Leo. "Optimization of a commercial aircraft environmental control system." Applied thermal engineering 22.17 (2002): 1885-1904.

[18] Silva, G. A. L., Silvares, O. M., and Zerbini, E. J. G. J., "Numerical Simulation of Airfoil Thermal Anti-ice Operation, Part 1: Mathematical Modelling," Journal of Aircraft, vol. 44, 2007, pp. 627–633.

[19] Scott K. Thomas, Robert P. Cassoni, and Charles D. MacArthur. "Aircraft anti-icing and de-icing techniques and modeling", Journal of Aircraft, Vol. 33, No. 5 (1996), pp. 841-854.

[20] Müller, Christian, Dieter Scholz, and Tim Giese. "Dynamic simulation of innovative aircraft air conditioning." DGLR: Deutscher Luft-und Raumfahrtskongress. Bonn: Deutsche Gesellschaft für Luft-und Raumfahrt (2007).

[21] Santos, A., Andrade, C., and Zaparoli, E., "A Thermodynamic Study of Air Cycle Machine for Aeronautical Applications," International Journal of Thermodynamics, vol. 17, 2014, p. 117.

[22] "Aviation Maintenance Technician Handbook - Airframe." Federal Aviation Administration, U.S. Department of Transportation 15 May 2014.

[23] Warrendale, "Ice, rain, fog, and frost protection," Society of Automotive Engineers, 1989.

[24] Linares, Daniel Perez, "Modeling and Simulation of an Aircraft Environmental Control System," École Polytechnique de Montréal, Aug. 2016.

[25] Sobieszczanski-Sobieski, Jaroslaw, and Raphael T. Haftka. "Multidisciplinary aerospace design optimization: survey of recent developments." Structural optimization 14.1 (1997): 1-23.

[26] R Perez, H Liu, and K Behdinan. "Evaluation of Multidisciplinary Optimization Approaches for Aircraft Conceptual Design," AIAA paper, Jan 2004.

[27] Talgorn, Bastien, et al. "Numerical investigation of non-hierarchical coordination for distributed multidisciplinary design optimization with fixed computational budget." Structural and Multidisciplinary Optimization 55.1 (2017): 205-220.

[28] Tosserams, S., et al. "A nonhierarchical formulation of analytical target cascading." Journal of Mechanical Design 132.5 (2010): 051002.

[29] Cebeci, Tuncer, and Fassi Kafyeke. "Aircraft icing." Annual review of fluid mechanics 35.1 (2003): 11-21.

[30] Al-Khalil, Kamel M., et al. "Validation of NASA Thermal Ice Protection Computer Codes. Part 3; The Validation of Antice." (2001).

[31] Paraschivoiu, I., P. Tran, and M. T. Brahmi. "Prediction of ice accretion with viscous effects on aircraft wings." Journal of aircraft 31.4 (1994): 855-861.

[32] Mingione, Giuseppe, and Vincenzo Brandi. "Ice accretion prediction on multielement airfoils." Journal of Aircraft 35.2 (1998): 240-246.

[33] Isight 5.9 Datasheet. Dassault Systemes, www.3ds.com/fileadmin/PRODUCTS-SERVICES/SIMULIA/RESOURCES/Isight-5.9-datasheet.pdf.